OHBAYASHI-GUMI
TECHNICAL RESEARCH INSTITUTE
ENVIRONMENTAL LABORATORY LETTER

Wind Tunnel Studies on Natural Air Flow Through Building

OHBAYASHI-GUMI, LTD.
Technical Research Institute
4-640, Shimokiyoto, Kiyose-shi, Tokyo, Japan
Tel : (0424) 91-1111

Wind Tunnel Studies on Natural Air Flow Through Building

0. PREFACE

Since the oil crisis, energy conservation and use of natural energy sources have become increasingly important factors when designing buildings. These factors are especially important in the field of building environmental controls, not only in practice but also in studies and they have been studied intensively. Given the recent cuts in oil prices, there exists no imminent energy crisis. However, the exhaustion of fossil energy resources is, nevertheless, taking place. Problems related to changeovers to other energy sources have not yet been solved. Under these circumstances, energy conservation and the use of natural energy sources are all the more important. Using artificial means to control building temperature is inevitably accompanied by air and thermal pollution. As long as fossil fuels are used, this takes place regardless of how efficient energy conservation measures are. Thus, the use of natural energy sources has significant meaning.

Using natural energy, warming rooms using solar energy used to be the most popular. As shown in the climograph, Fig.1, almost all regions in Japan require measures to cope with both cold and heat. Summers in Japan are hot and humid and winters are cold and dry. Compared with heating, it is extremely difficult to utilize natural energy for cooling. With today's technology, we can only use diurnal and nocturnal temperature differences to store coolness or use the cooling effects of water evaporation. However, given Japan's hot and humid summer, great expectations can not be placed on water evaporative cooling. Storing coolness is also difficult due to condensation.

The usual methods for cooling hot rooms are sun shading and natural air flow. This can lower the indoor temperature to that of the outdoor air. In addition, the development of techniques that produce a cooling feeling, namely to lower effective temperature, is much sought after. This can be done using natural air flow.

This paper deals with studies on the indoor natural air flow in buildings in the search to minimize room temperature rises while permitting air movement which produces a cooling sensation.

1. PAST STUDIES ON NATURAL AIR FLOW

Studies on indoor air flow caused by wind can be divided into the following three categories:

1) Behavioral studies on visualized air streams
2) Calculating air flow rate by expanding the calculation method for the ventilation caused by natural wind
3) Model experiments and measurements with respect to wind speed coefficients

Among past studies, some studies worthy of mention are Olgyay's /1/ relating to 1), Ishihara's /2/ and Kodama's /3/ to 2), and Aynsley /4/ and Ishihara's /5/ to 3). The results of these works chiefly center on single rooms and there are limitations in their application and quantification. Applying them to practical use calls for experiments on a case-by-case basis. However, the results have been put on use for comparative and design studies in the design stages. This is because they offer means for qualitative understanding as well as some limited degree of quantifications.

In our studies, we conducted experiments using 5 scaled-down models of houses attached together and placed in a smoke wind tunnel. The quantitative as well as qualitative studies were achieved by visualizing the air flow in the wind tunnel.

Apartment buildings are growing in number and this trend will continue for some time in the future. Use of natural wind for such apartments is not easy since benefit from natural wind differs from one apartment to another due to differences in height as well as in position from the gable side. The availability of apertures limited only to the walls opposite each other also makes the use of natural wind more difficult than in the case of detached houses.

2. SUMMARY OF EXPERIMENTS

Fig.2 shows models used for the experiments. The models are made of transparent acrylic board with a thickness of 3mm. Five units each of the identical models were made available for simulations of plane figures as well as five-story section figures of five-household housing aggregations. The plane figures include a rectangular plane composed of a. in Fig.2, as well as a zig-zag plane composed of b. shown in Fig.2. The section figures include an upright section composed of a. as well as a setback section composed of b. For the plane figures, studies were conducted on apertures having different dimensions and shapes as shown in Table-I.

Fig.3 shows a schematic figure of the smoke wind tunnel used. Its measurement platform measures 600 x 1,000 x 250mm and one side is transparent to permit observation. Smoke is discharged from 30 nozzles, each smoke trail has a diameter of 1 to 2mm.

To secure sufficient two-dimensionality, a camera was placed approximately 8m away from the transparent observation window and a telescopic objective lens with a 200mm focal length was used for photographing. Pictures were taken at an f number of 5.6 and shutter speeds of 1/8 and 1/4 sec. ASA 400 film was used and was then 4x-hypersensitized during development. Fig.4 shows an experiment using models for upright section measurement.

3. PRELIMINARY EXPERIMENTS - SIMILARITY STUDIES

The wind tunnel air flow velocity at which smoke trails are most clearly seen is 3.6m/sec. Experiments were conducted at various air stream velocities. Fig.5 shows their results. As shown, no difference was recognized in the air stream over the experimented velocity range. Experience has confirmed that similar air stream behavior can be obtained as long as turbulence is sufficiently developed around subjects having abrupt edges. At the optimum air stream velocity and by converting the longer side of a unit house to present the characteristic length, the Re value can be obtained by the calculation given below. Since the value obtained indicates a sufficient turbulence development, the results of the experiments can be applied to actual designs for buildings having arbitrary sizes as well as to other velocities.

$$R_e = \frac{3.6 \times 0.25}{1.483 \times 10^{-5}} = 6.1 \times 10^4$$

4. RESULTS OF EXPERIMENTS ON PLANE FIGURES

4.1 Wind direction and air flow rate :

Partial results obtained from the plane figures are shown in Fig.6 and Fig.7.

4.1.1 Air flow rate determined by the number of smoke trails

Air flow rates can be determined by the number of smoke trails recorded on the photographs. Since all the smoke trails within S_o as shown in the schematic Fig.8 are considered to pass through the building, the air flow rate $Q_1(\theta_w)$ as well as the ratio of the air flow rates $\eta(\theta_w)$: $Q_1(\theta_w)$ to $Q_1(0)$, at a natural wind velocity of V_o and its incidence angle of θ_w, can be obtained by equations (1) and (2). Where $S_o(0)$ and $S_o(\theta_w)$ are S_o values corresponding to respective angle of wind incidental to the building: 0 degree and θ_w degrees.

$$Q_1(\theta_w) = S_o(\theta_w) \cdot V_o \tag{1}$$

$$\eta(\theta_w) = Q_1(\theta_w)/Q_1(0) = S_o(\theta_w)/S_o(0) \tag{2}$$

4.1.2 Projected area on wall surface Sm against natural wind: $S_p(\theta_w)$

i. In case of rectangular planes

$$S_p(\theta_w) = S_m \cdot \cos\theta_w \tag{3}$$

$$R(\theta_w) = S_p(\theta_w)/S_m = \cos\theta_w \tag{4}$$

ii. For zigzag planes

$$S_p(\theta_w) = \pm S_m \cdot \left\{\cos\theta_w - (\sin\theta_w)/2\right\} \tag{5}$$

$$R(\theta_w) = \pm\left\{\cos\theta_w - (\sin\theta_w)/2\right\} \tag{6}$$

where the symbol + is $-90° < \theta_w < \tan^{-1} 2$

\- is $\tan^{-1} 2 < \theta_w < 90°$

4.1.3 Air flow rate calculated using wind pressure coefficient

$$Q_2(\theta_w) = 5 \cdot V_o \sqrt{\left\{C_w(\theta_w) - C_L(\theta_w)\right\}/K} \tag{7}$$

$$K = 1/(\alpha_w \cdot A_w)^2 + 1/(\alpha_L \cdot A_L)^2$$

$$\delta(\theta_w) = Q_2(\theta_w)/Q_2(0) = \sqrt{\left\{C_w(\theta_w) - C_L(\theta_w)\right\}/\left\{C_w(0) - C_L(0)\right\}} \tag{8}$$

where,

$C_w(\theta_w)$ and $C_L(\theta_w)$ are the respective windward and leeward wind pressure coefficients when the incidence angle of the natural wind is θ_w degrees.
α and A are the flow coefficient and the area of the aperture respectively.

Subscripts: w; for windward and L; for leeward

Fig.9 shows values for $\eta(\theta_w)$, $R(\theta_w)$ and $\delta(\theta_w)$ obtained by experiments

8 and 15 in Table I. Since a wind pressure coefficient could not be obtained for the zigzag plane, the $\zeta(\theta_w)$ shows the results of the experiment 8 only. Wind pressure coefficients in Table II are used. As figure clearly shows, the changes in air flow rate in relation to wind direction, determined by the number of smoke trails, almost identically correspond to the changes of projected area. Air flow rates obtained by calculations with wind pressure coefficients tend to become larger than the ones in the former two cases at larger wind incidence angles ($\theta_w > 60°$). Calculated air flow rates are thus excessively large under such conditions. A small aperture provided for each model housing unit in comparison with the interval of smoke trails did not permit the determination of differences in air flow rate from unit to unit.

4.2 Aperture shapes and air flow rates

To determine optimum shapes and dimensions of the apertures for the maximum intake of natural wind, how S_o undergoes changes with respect to wind directions is shown in Fig.10 and Fig.11.

4.2.1 Aperture sizes and air flow rate

For rectangular plane figures, comparisons between experiments 2 and 4 as well as between 3 and 5 in Fig.10 were made.

When,
Natural wind incidence $\theta_w < 60°$: The greater the aperture ratio, the greater the air flow rate.
Natural wind incidence $\theta_w > 60°$: Air flow rate decreases abruptly at guide vane angles other than 45° and the influence of aperture ratio differences decreases.

For zigzag plane figures, comparison between the experiments 10 and 12 as well as between 11 and 13 in Fig.11 were made.
When,
$-75° < \theta_w < 45°$: The greater the aperture ratio, the greater the air flow rate.
$\theta_w < -75°$, $\theta_w > 45°$: Air flow rate decreases abruptly and the influence of aperture ratio differences decreases.

4.2.2 Guide vane angles and air flow rates

For rectangular plane figures, comparisons between experiments 2, 3 and 6 as well as between 4, 5 and 8 in Fig.10 were made.

When,
$\theta_w < 60°$: Almost no difference in air flow rates between no guide vane and with guide vane set at 90°. Poor results obtained with guide vane at 45°.
$\theta_w > 60°$: Abrupt decreases without guide vane. Guide vane set at 45° yielded best results.

For zigzag plane figures, comparisons between experiments 10, 11 and 14 as well as between 12, 13 and 15 in Fig.11 were made.
When,
$-75° < \theta_w < 45°$: Best results obtained without guide vane and better re-

sults at 90° then 45° guide vane angles.

$\theta_w < -75°$, $\theta_w > 45°$: Abrupt decreases without guide vane and better results achieved at 45° guide vane angle.

4.2.3 Air flow rate with respect to plane figure

When,

$-90° < \theta_w < 15°$: Better results with zigzag planes

$15° < \theta_w < 45°$: Less differences between both planes and they decrease abruptly as natural wind incidence angle becomes larger.

On the whole, zigzag planes were most advantageous. For rectangular planes, over the range of $-90° < \theta_w < 0°$, the same tendencies as obtained in the experiment 2 were assumed.

4.3 Wind speed coefficient

Generally the definition of wind speed coefficient refers to the ratio of airstream velocity to natural external wind velocity /7/ measured at an arbitrary point in a room. However, in this paper, the wind speed coefficiency is defined as the ratio of the average wind velocity at windward aperture to the average natural wind velocity. Using equation (1), wind speed coefficient $\varphi(\theta_w)$ may be expressed in the following equation (9).

$$\varphi(\theta_w) = \{S_o(\theta_w) \cdot V_o / S_m\} / V_o = S_o(\theta_w) / S_m \qquad (9)$$

How $\varphi(\theta_w)$ undergoes changes with respect to wind directions is shown in Fig.12 and Fig.13.

4.3.1 With guide vane set at 90° and without

Comparisons between experiments 2 and 4, 6 and 8, 10 and 12 as well as 14 and 15 were made. As figure explicitly shows, as the aperture ratio becoems smaller, the wind speed coefficient becomes larger.

4.3.2 With guide vane set at 45°

For rectangular planes, a comparison between experiments 3 and 5 was made. Irrespective of aperture ratios, wind speed coefficients become constant.

For zigzag planes, a comparison between experiments 11 and 13 was made.

When, i) $\theta_w < -45°$ and $0° < \theta_w < 60°$: The smaller the aperture ratio, the greater the wind speed coefficient.

ii) $-45° < \theta_w < 0°$ and $\theta_w > 60°$: The greater the aperture ratio, the greater the wind speed coefficient.

Generally, decreasing the aperture size will increase the wind speed coefficient. However, in the case of ii) the wind speed coefficient becomes smaller. This is thought to be caused by the guide vane itself since it may create large resistance to the air flow decreasing the flow rate when the aperture is decreased in size.

5. RESULTS OBTAINED ON SECTIONS (Fig.14)

Comparisons were made only between upright and setback sections. Larger air flow rates were achieved for the upright section when the guide vane was set at 90°. However, almost the same results were obtained without a guide vane.

6. SUMMARY

Air flow rates obtained by calculating using wind pressure coefficients tend to become excessively larger as the degree of parallelism between the natural wind and the apertures increases. To increase air flow rate, apertures may be enlarged.

For zigzag plane figures, adjoining houses' walls are more effective than guide vanes and the zigzag plane figures are, as a whole, more advantageous over the others.

The effectiveness of guide vane becomes more apparent as the parallelism between the natural wind and the apertures increases.

To increase indoor air movement velocity, apertures may be down sized if there is no guide vane or when guide vanes are set at 90°.

At a guide vane angle of 45°, if the aperture size is almost the same as the guide vane, the guide vane works as resistance and its use is disadvantageous.

7. REFERENCES

/1/ V. Olgyay: Design with Climate, Princeton Univ. Press, Princeton, 1963

/2/ Masao Ishihara: Experimental Studies on Natural Air Flow, Trans. of the Architectural Institute of Japan, No.21, Tokyo, 1953

/3/ K. Seike, U. Kodama, N. Takada: Influences of Room Shape on Natural Air Flow (1), (2), (3), Proceedings of Annual Meeting of Architectural Institute of Japan, (Planning Section), Tokyo, 1977, 1978

/4/ R.M. Aynsley: Architectural Aerodynamics, Applied Science Publishers Ltd., London, 1977

/5/ Masao Ishihara: Air Speed and Its Direction in Room Caused by Wind, Tans. of the Architectural Institue of Japan, No.54, Tokyo, 1956

/6/ Pamphlet of the Architectural Institute of Japan No.18; Ventilation Design, the Architectural Institute of Japan, Tokyo, 1965

/7/ K. Sato: Planning of Ventilation and Air Flow, Series of Architecture No.22, Shokokusha, Tokyo, 1957

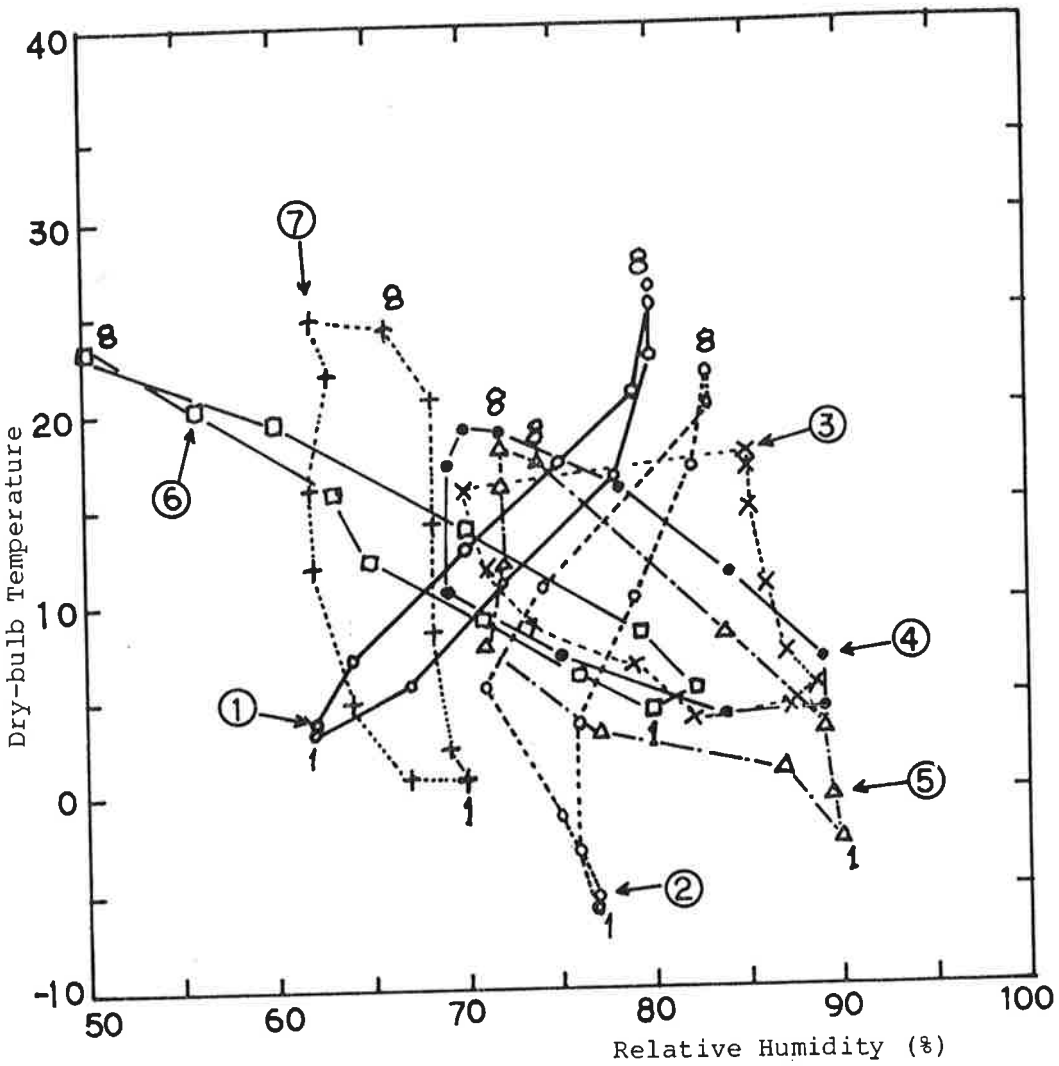

Fig.1 Climograph

1 - Tokyo
2 - Sapporo
3 - London
4 - Paris
5 - Munich
6 - Madrid
7 - New York

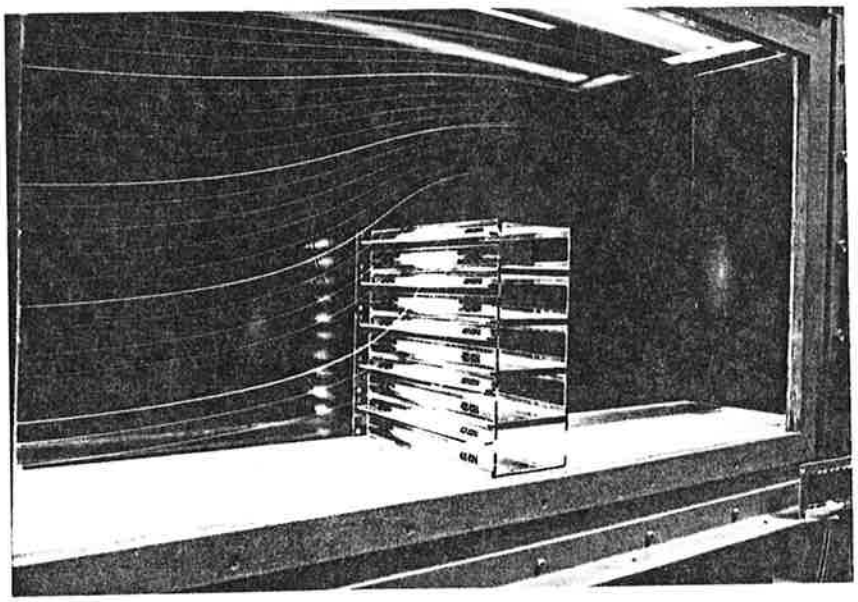

Fig.4 Stream Line in Smoke Wind Tunnel

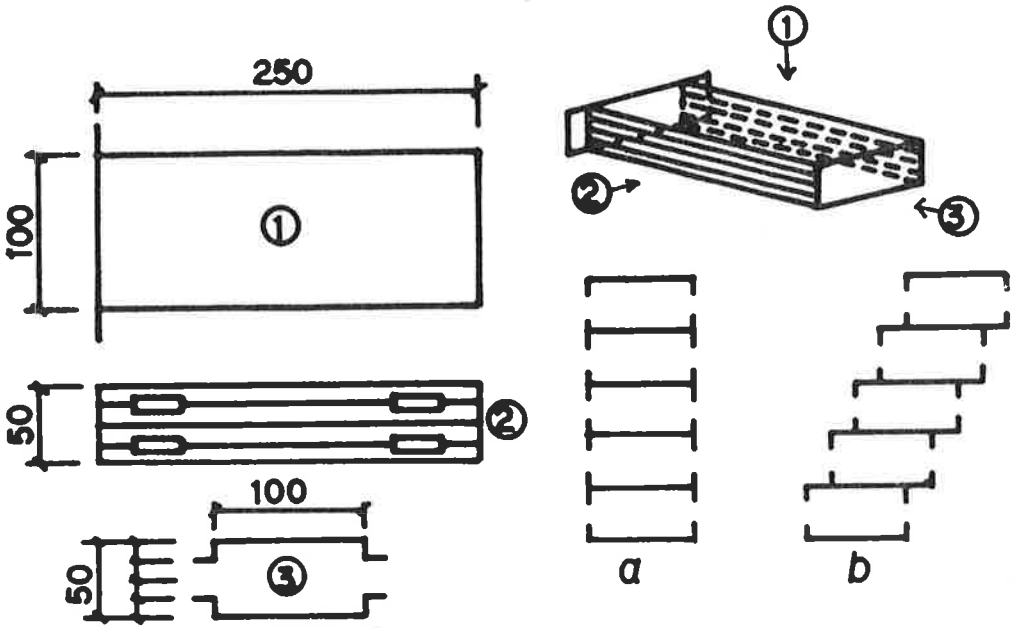

Fig.2 Model Building

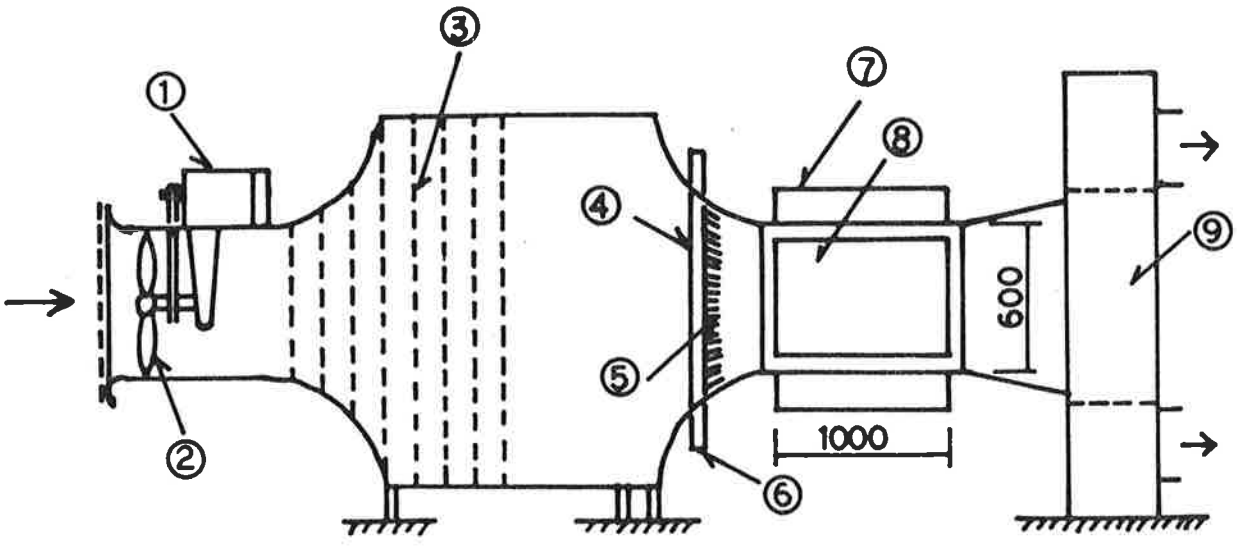

Fig.3 Smoke Wind Tunnel

1 - Motor
2 - Fan
3 - Meshes
4 - Symmetric Wing
5 - Smoke Nozzle
6 - Smoke Inlet
7 - Light (Tungsten-Halogen)
8 - Observing Wind (Glass)
9 - Exhaust Duct

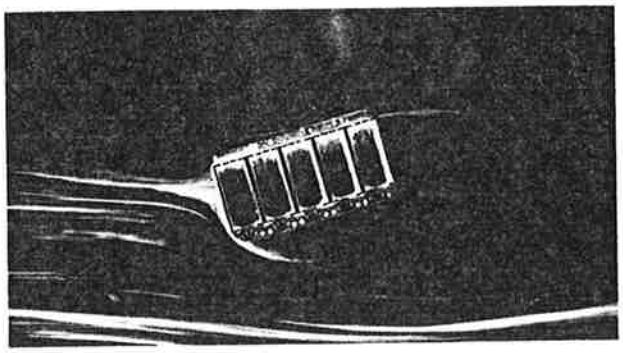

Fig.5-a Velocity = 0.8m/s

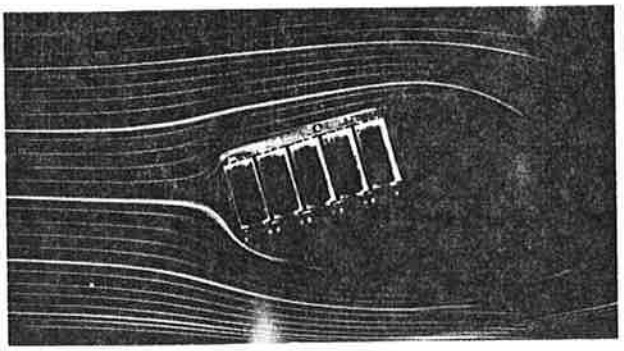

Fig.5-b Velocity = 1.95m/s

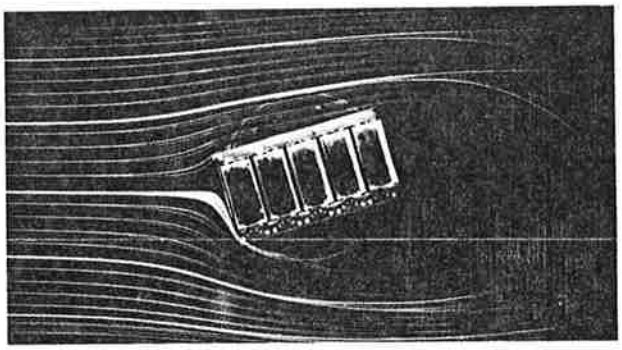

Fig.5-c Velocity = 3.18m/s

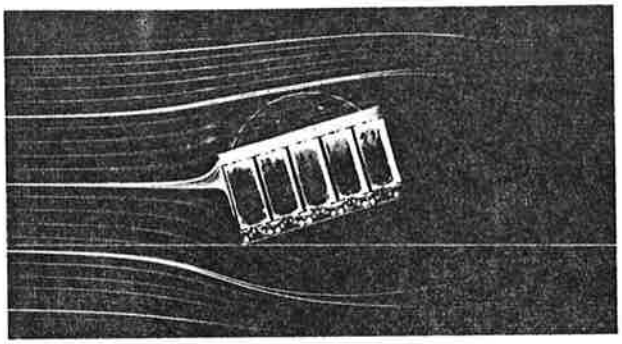

Fig.5-d Velocity = 3.90m/s

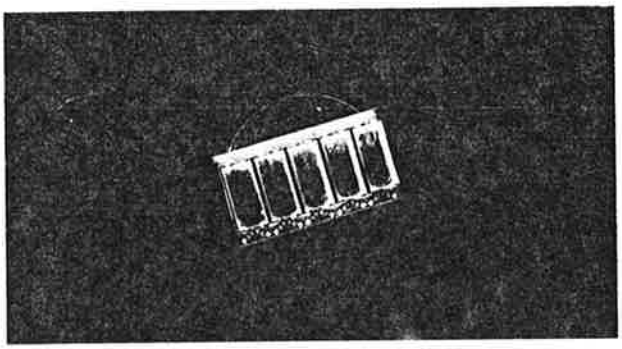

Fig.5-e Velocity = 6.06m/s

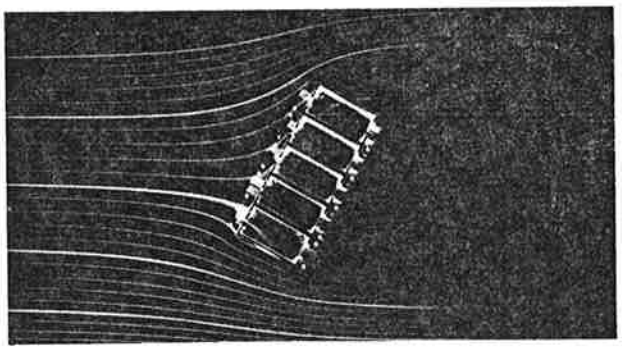

Fig.6-a Rectangular Plane
w=1/4, No GV, θw=30°

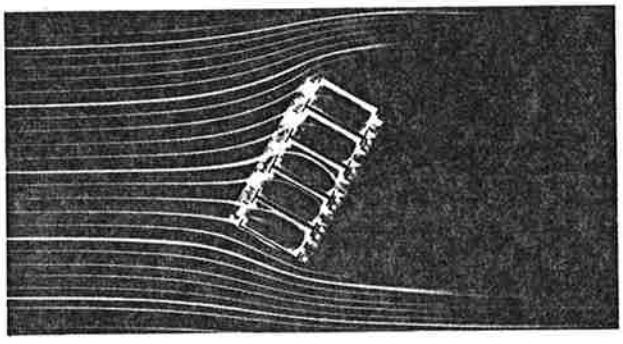

Fig.6-b Rectangular Plane
w=1/2, GV=90°, θw=30°

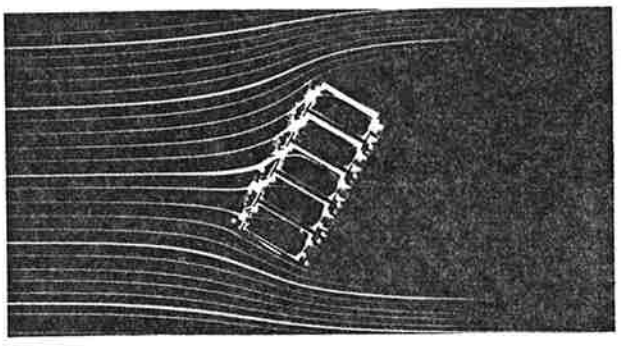

Fig.6-c Rectangular Plane
w=1/2, GV=45°, θw=30°

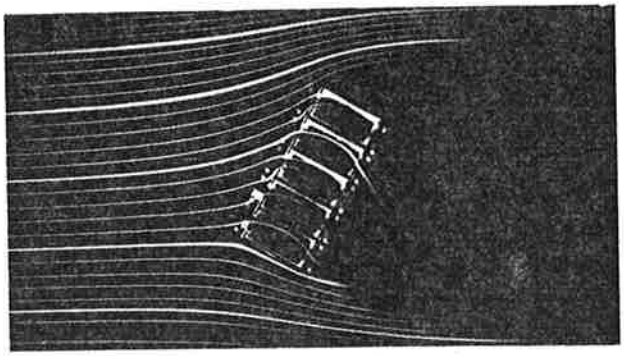

Fig.6-d Rectangular Plane
w=½, No GV, θw=30°

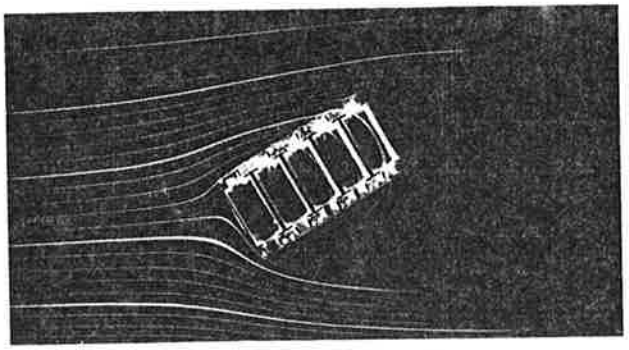

Fig.6-e Rectangular Plane
w=½, GV=90°, θw=60°

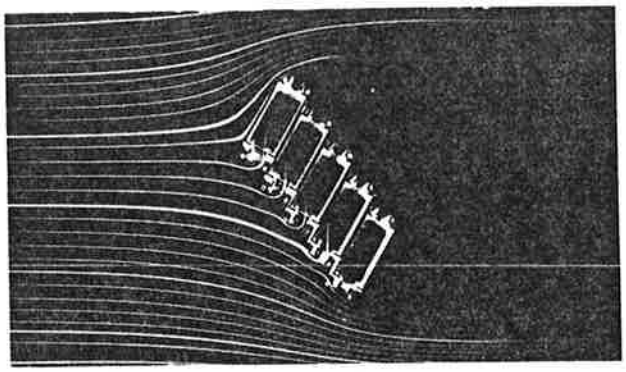

Fig.7-a Zigzag Plane
w=½, GV=90°, θw=-60°

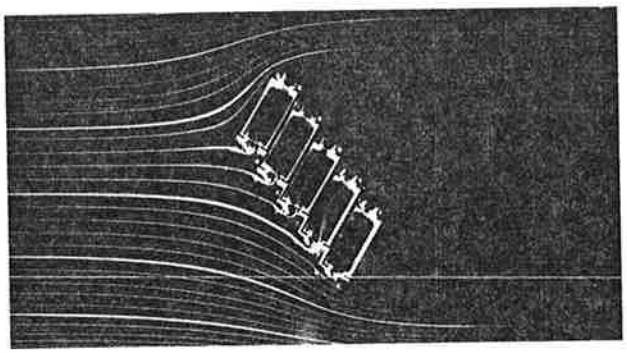

Fig.7-b Zigzag Plane
w=½, GV=45° θw=60°

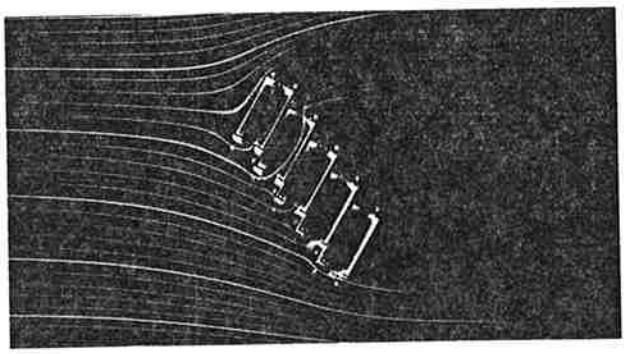

Fig.7-c Zigzag Plane
w=½, No GV, θw=60°

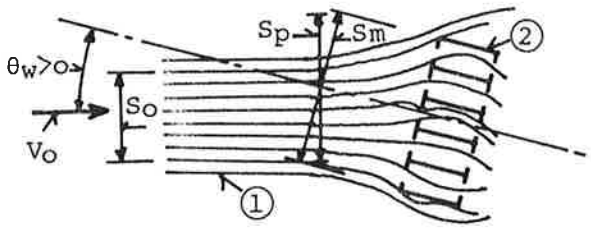

Fig.8 Schematic Diagram
of Stream Lines

1 - Stream Lines
2 - Model Building

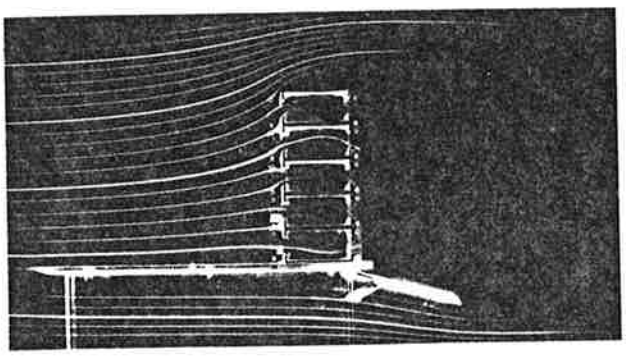

Fig.14-a Upright Section

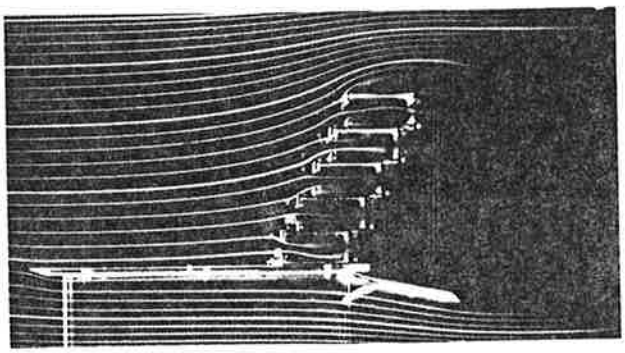

Fig.14-b Set-back Section

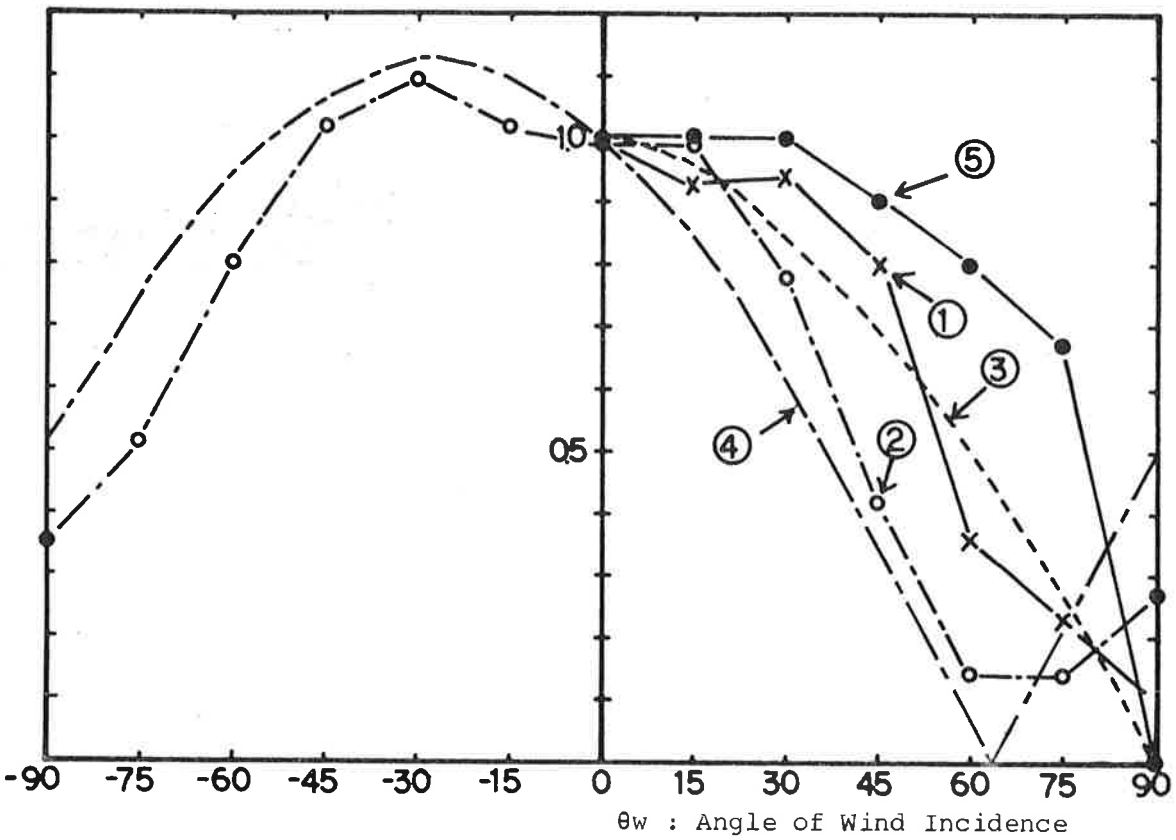

Fig.9 Comparison with Flow Rate

1 - Air Flow Rate Obtained by Stream Line (Rectangular Plane)

2 - Air Flow Rate Obtained by Stream Line (Zigzag Plane)

3 - Projection Area (Rectangular Plane)

4 - Projection Area (Zigzag Plane)

5 - Calculated Value Using Wind Pressure Coefficient

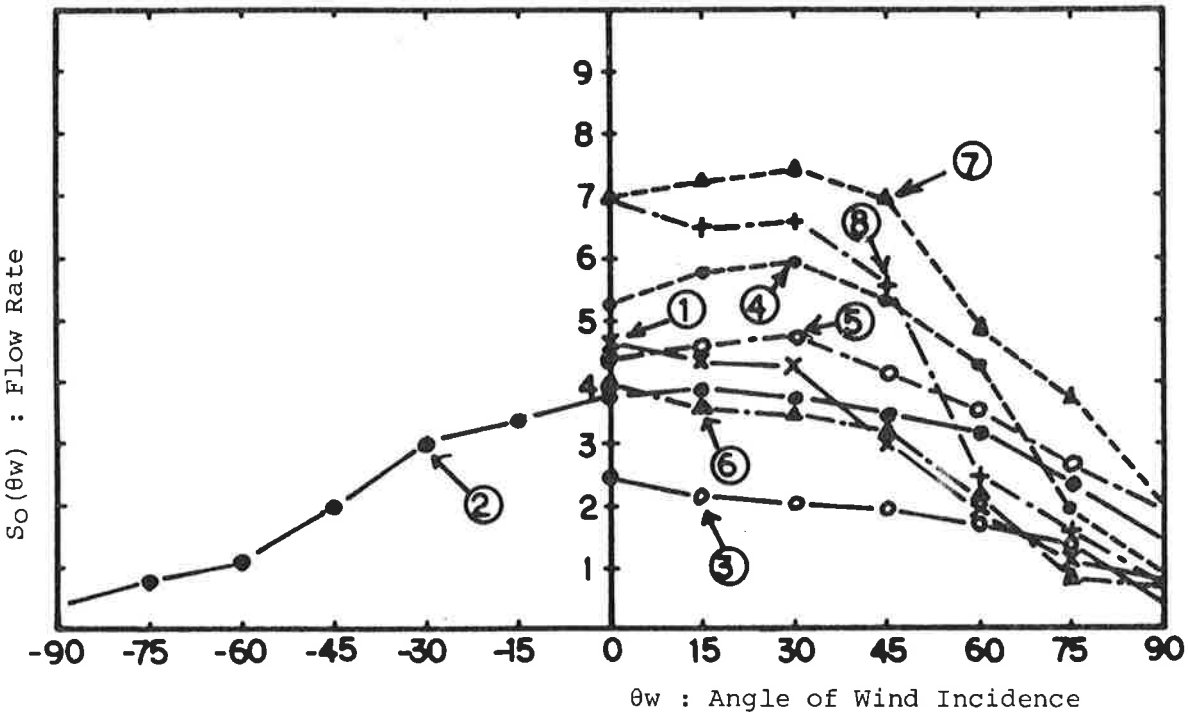

Fig.10 Flow Rate by Stream Line (Rectangular Plane)
N.B Graph No. is case of Experiment

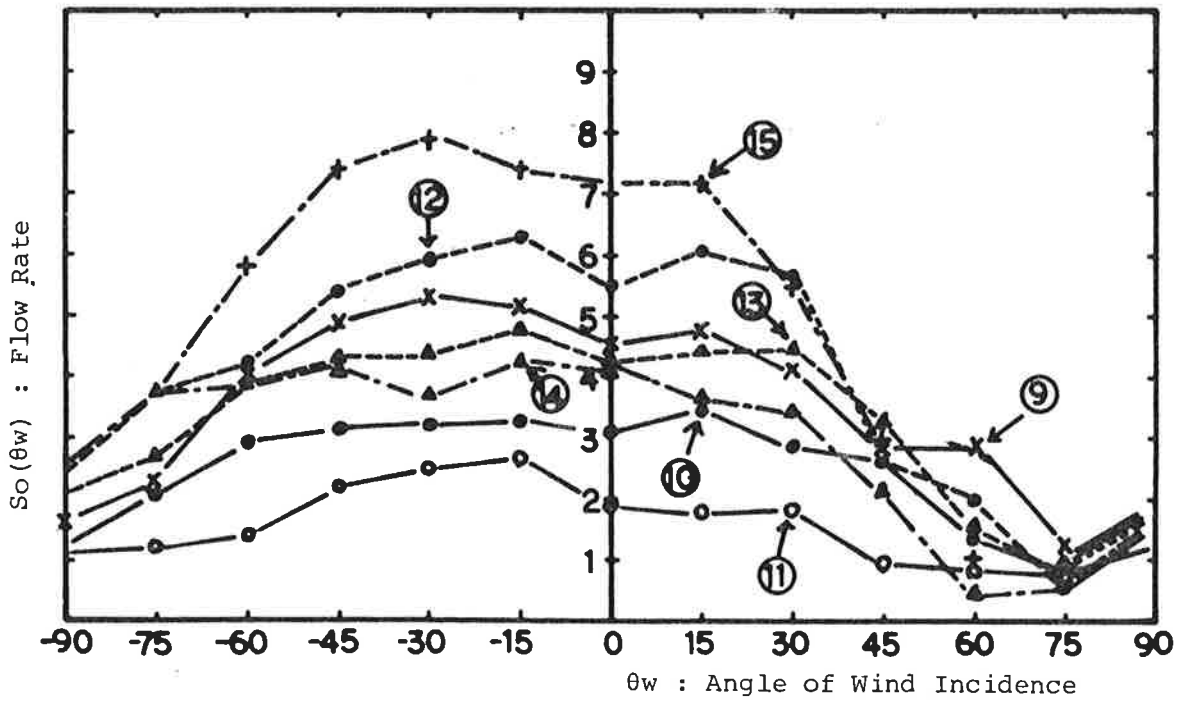

Fig.11 Flow Rate Stream Line (Zigzag Plane)

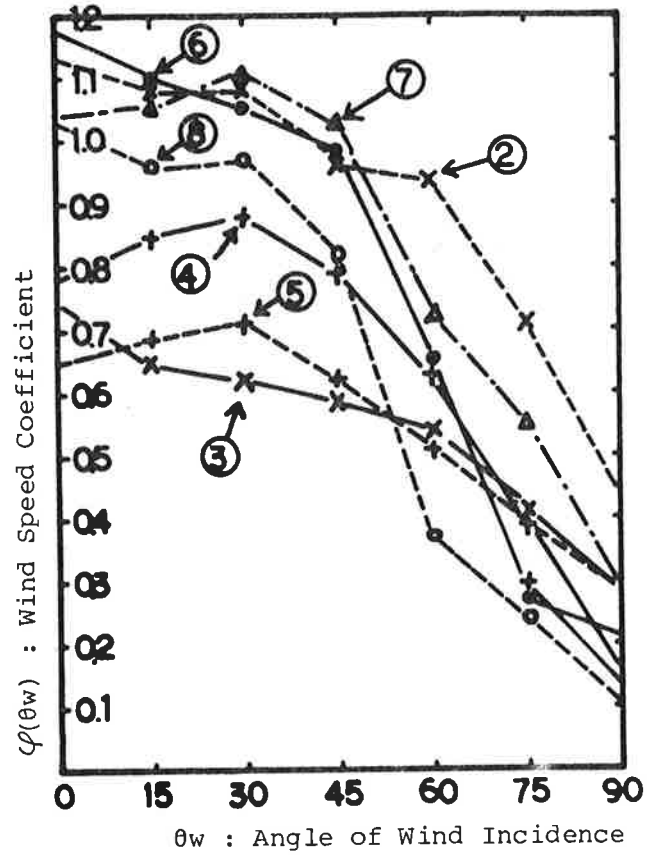

Fig.12 Wind Speed Coefficient (Rectangular Plane)

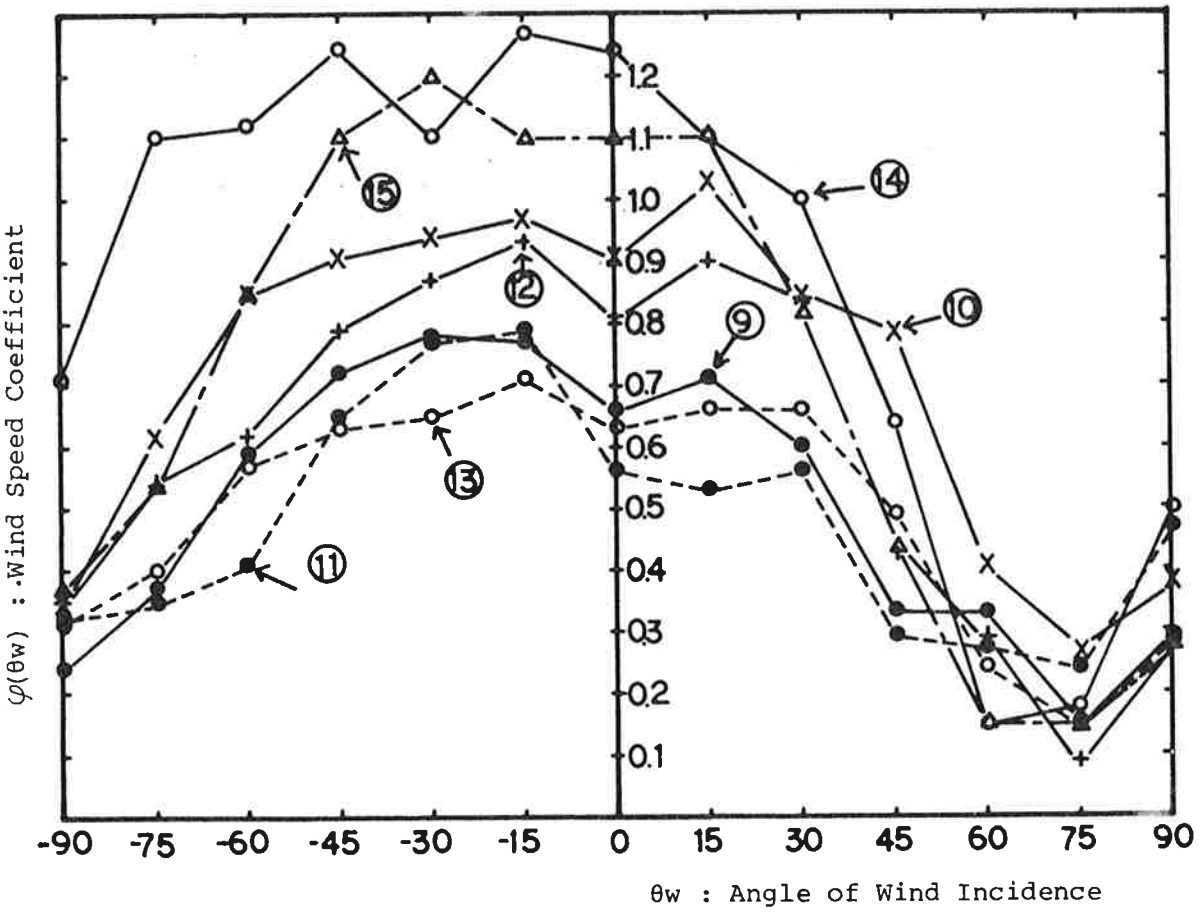

Fig.13 Wind Speed Coefficient (Zigzag Plane)

Table-I Case of Experiments

No	Rectangular Plane		No	Zigzag Plane	
1	GV = 90° W = 1/2	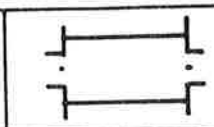	9	GV = 90° W = 1/2	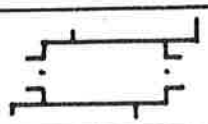
2	90° 1/4	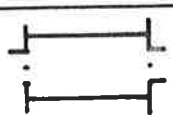	10	90° 1/4	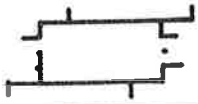
3	45° 1/4	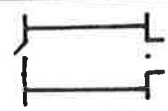	11	45° 1/4	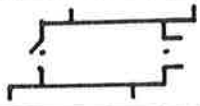
4	90° 1/2		12	90° 1/2	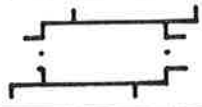
5	45° 1/2		13	45° 1/2	
6	No 1/4	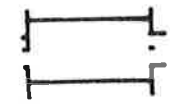	14	No 1/4	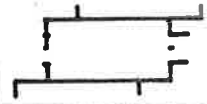
7	90° 1/2		15	No 1/2	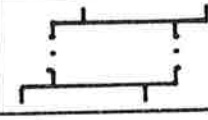
8	No 1/2		GV ; Angle of Gide-Van W ; Rate of Opening		
	Upright Section			Set-back Section	
16	GV = 90, W = 1/4		18	GV = 90, W = 1/4	
17	No W = 1/2		19	No W = 1/2	

Table-II Wind Pressure Coefficient

Angle of Wind Incidence	0°	15°	30°	45°	60°	75°	90°
Windward	0.75	0.76	0.75	0.43	0.25	0.0	-0.44
Leeward	0.40	-0.50	-0.49	-0.50	-0.49	-0.52	-0.44